Solution-Based Growth and Optical Properties of Self-Assembled Monocrystalline ZnO Ellipsoids

Jinping Liu,[†] Xintang Huang,*[,†] K. M. Sulieman,[†] Fenglou Sun,[‡] and Xiang He[‡]

Department of Physics, Central China Normal University, Wuhan 430079, P R China, and Plasma Institute, South-Central University for Nationalities, P R China

Received: November 27, 2005; In Final Form: April 11, 2006

Self-assembled unusual ZnO ellipsoids have been grown by a facile low-temperature (60 °C) solution process on a large scale. FESEM and TEM reveal that these ellipsoids have an average horizontal axis of 1.5 μm and a longitudinal axis of 0.6 μm. Experimental results obtained from the early growth stage demonstrate that the ZnO ellipsoidal structures are single crystals and formed from direct "oriented attachment" of two types of building blocks, that is, nanorods and nanoparticles. It is further found that the existence of poly(ethylene glycol) (PEG-10 000) is vital to the formation of the complex microparticles. Raman spectrum, room-temperature photoluminescence, and UV−vis absorption spectra are also discussed. This work presents a simple and effective route for large-scale fabrication of single-crystal ZnO ellipsoids with micrometer-scale sizes and 3D self-assembled structures.

Introduction

Recent efforts have produced significant advances in the fabrication of size- and shape-controllable nanostructures. Further efforts have been directed to the studies of the optical, magnetic, and electronic properties of these materials. ZnO is a versatile semiconductor material with excellent properties and extensive applications in electronics, photoelectronics, sensors, and catalyses.[1−3] It is well known for its wide band gap (3.37 eV) and high exciton binding energy at room temperature (60 meV).[3,4] Yang's research group observed the room-temperature UV-lasing from ZnO nanorod arrays in 2001,[4] which has enabled a wide range of research interest in searching for new synthetic methods of ZnO nanostructures with high quality and various exciting morphologies. For ZnO, 1D, 2D, and 3D structures including nanowires, nanorods, nanotubes, nanobelts, nanosaws, nanosheets, nanorings, and tetrapodlike patterns have been reported successfully.[3−8] To prepare these nano/microstructures, physical methods such as chemical vapor deposition (CVD), thermal evaporation, and template-directed growth are generally used. However, most of the routes have employed high temperatures or special complex processes, which is unfavorable for low-cost and large-scale production. It is believed that solution methods (SM), which are appealing for their facile manipulation and potential for scale-up, could solve this problem; and the recent reports,[9−15] for example, synthesis of ZnO helical rods,[10] disks,[11] flowerlike aggregates,[13] rotorlike structures,[14] and hollow microhemispheres/microspheres,[15] have proven the convenience and simplicity in the fabrication of ZnO nanostructures by SM, especially of 3D self-assembled ZnO structures.

Ordered self-assembly of nanoscale building blocks, such as nanoparticles, nanoribbons, nanorods, and so forth, into various single-crystalline architectures has become a hot topic in recent material research fields.[9,16−25] This process seems very promising as a route for the preparation of complex-shaped nanostructures through the "oriented-attachment" mechanism.[9] Understanding the control factors for creating nanocrystal assemblies would allow the design of desired nano/microstructures for potential applications in optical, electronic, chemical, and biological fields. To our knowledge, most of the reported literature related to the oriented aggregation concentrated on the self-assembly of limited number of nanoparticles into one-dimensional (1D)[9,16,17,19−22] or two-dimensional (2D)[18,23,24] crystalline nanostructures. At the beginning of this year, three-dimensionally oriented aggregation of a few hundred CuO nanoparticles into monocrystalline architectures with nanoscale sizes was realized.[25] In that regard, selective adsorption and subsequent controlled removal of organic additives (formamide) at interfaces played important roles in rotating adjacent nanoparticles so that they shared an identical 3D crystallographic orientation. Because there is almost no research on the self-assembly of different kinds of building blocks into 3D single-crystalline microarchitectures, it is our goal to observe and understand the 3D oriented-attachment process of more than one kind of nanobuilding block into larger single-crystalline materials by a simple route. Herein, we report the first large-scale synthesis of unusual ZnO ellipsoids by a facile solution process. The synthetic strategy is based on the oriented-attachment mechanism in the presence of PEG-10 000, involving a low temperature (60 °C), simple reaction devices, and low-cost starting materials. The created ellipsoids are essentially different from the well-known nanorods, nanowires, nanotubes, nanobelts, and nearly spherical morphologies that are obtained by the common Ostwald ripening process. It was found that the ellipsoidal structures with micrometer-scale sizes exhibit relatively uniform morphology, rough surfaces, and good single-crystalline characteristics. Moreover, they are interestingly composed of two types of building blocks, namely, 1D nanorods and zero-dimensional (0D) nanoparticles, which is also unique in comparison with ZnO nanostructures formed by assembly of only nanoparticles.[9] The optical properties of these ZnO

* To whom correspondence should be addressed. Fax +86-027-67861185; e-mail: xthuang@phy.ccnu.edu.cn.
[†] Central China Normal University.
[‡] South-Central University for Nationalities.

10.1021/jp056880r CCC: $33.50
Published on Web 05/17/2006

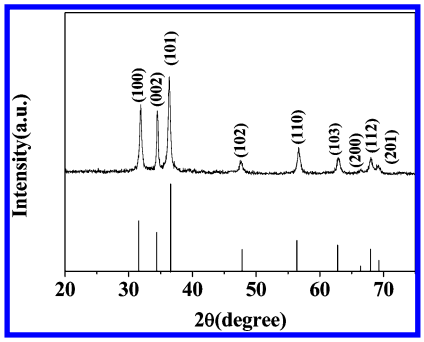

Figure 1. XRD pattern of the as-prepared ZnO ellipsoids.

ellipsoids are also discussed. The study of luminescence property might shed some light on defects in the ZnO microstructures and their potential as photonic materials.[15] These complex assembled ZnO ellipsoids might be used in studies considering the effects of spatial orientation and arrangement of 0D and 1D nanosized building blocks on their collective catalytic, sensing, piezoelectric, and optoelectronic properties.

Experimental Section

All of the reagents used in the experiments were in analytical grade and utilized without further purification. To grow the ZnO ellipsoids, we used $Zn(NO_3)_2 \cdot 6H_2O$ and $NH_3 \cdot H_2O$ as the starting materials. First, 200 mL of 0.05 M $Zn(NO_3)_2$ aqueous solution was prepared in a beaker under stirring. A solution containing 0.85 M $NH_3 \cdot H_2O$ and 0.15 g of poly(ethylene glycol) (PEG-10 000) was prepared at room temperature. Then, the later solution was added dropwise to the former one. After the addition was finished, the obtained suspension (pH $\approx$ 7.5) was subsequently heated to 60 °C and kept reacting at this constant temperature under vigorous magnetic stirring for 1 day. The white powders collected from the bottom of the beaker were washed with absolute alcohol and distilled water, dried in vacuum for several hours, and kept for further characterization.

The phase purity of the as-prepared products was characterized by X-ray powder diffraction (XRD) using a Y-2000 X-ray diffractometer with Cu Kα radiation (λ = 0.15418 nm). The Raman spectrum was obtained on a Renishaw 1000 Raman spectroscope (Ar ion laser, 514.5 nm). Scanning electron microscopy images (SEM) were obtained on a JEOL JSM-6700F microscope operated at 5 kV. Transmission electron microscopy observations (TEM, HRTEM) were carried out on a JEOL JEM-2010 in bright field and selected area electron diffraction modes and a HRTEM JEM-2010FEF (operated at 200 kV). Room-temperature UV−vis absorption and photoluminescence (PL) spectra were recorded on a UV-2550 spectrophotometer and a continuous wave (cw) He−Cd (325 nm) laser, respectively.

Results and Discussion

Structure and Morphology. The XRD pattern of the as-prepared product (Figure 1) demonstrates that all of the diffraction peaks can be indexed to a pure wurtzite structure of ZnO with cell constants of a = 0.324982 nm and c = 0.520661 nm (JCPDS card no. 36-1451). No diffraction peaks from impurities are found in the sample within the experimental error. It is noticed that the intensity of the (002) peak is slightly stronger compared with that in the standard diffraction pattern, indicating that the structure of ZnO ellipsoids might have a preferential orientation along the c axis.

Figure 2a shows a typical SEM image of the self-assembled ZnO products. It can be seen clearly that ZnO ellipsoid-like

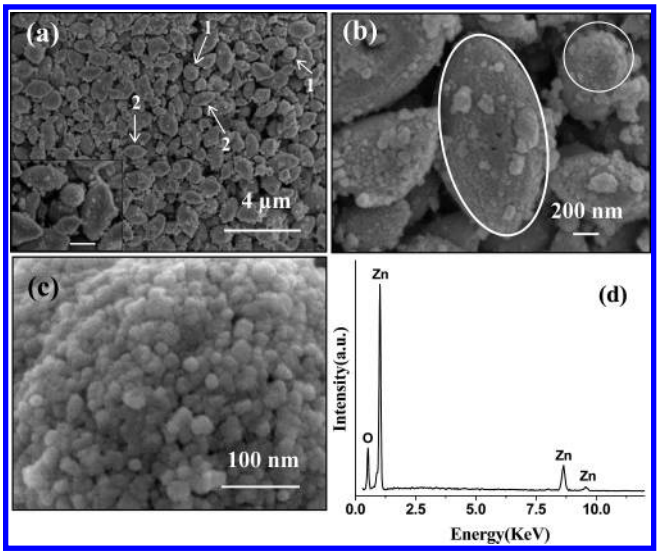

Figure 2. (a) Low-magnification image of large-scale self-assembled ZnO ellipsoids dispersing harmoniously. The scale bar in the inserted picture is 600 nm. (b) Enlarged image of an individual ZnO crystal showing standard ellipsoidal shape. (c) Particle-assembled surface image of ZnO ellipsoids. (d) EDS result of the ZnO ellipsoids.

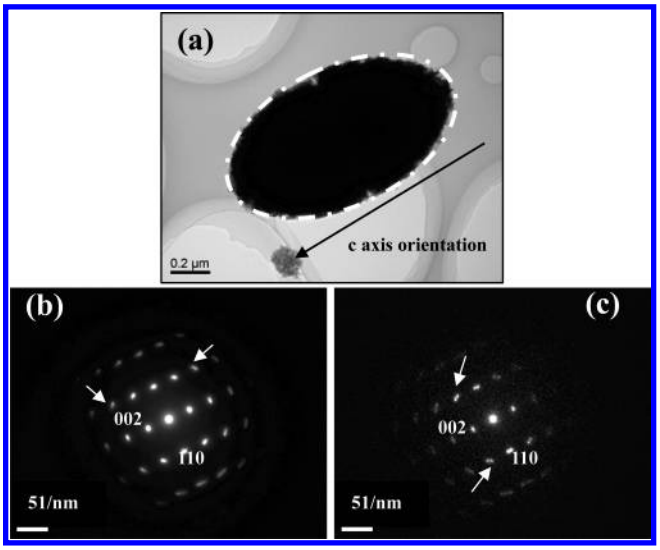

Figure 3. (a) TEM image of an individual ZnO ellipsoid. (b) The corresponding SAED pattern taken from the whole ellipsoid. (c) SAED pattern taken from one-half of the ellipsoid. The small white arrows in b and c indicate that some diffraction spots are broadened and elongated.

patterns, with the average horizontal axis of 1.5 μm and longitudinal axis of 0.6 μm, are obtained on a large scale. The ellipsoid-like shape is confirmed by the circular cross-sections observed from the vertically aligned ZnO micrometer-particles and the elliptical cross-sections detected from the horizontally dispersed micrometer-particles (see arrows 1 and 2 and the insert of Figure 2a). An individual ZnO micrometer-particle (Figure 2b) usually exhibits a standard geometrically ellipsoidal structure with a rough surface. At a higher magnification, apparently particle-assembled surfaces of some ZnO ellipsoids are observed (Figure 2c). The nanoparticles serving as building blocks are in the quasi-spherical shape and about 10−20 nm in diameter. On the basis of the above results, we conclude that the surfaces of these ellipsoids are formed from attachment of nanoparticles. It is noteworthy to stress that these ellipsoidal structures are sufficiently stable that they could not be destroyed even after long-time ultrasonication. From Figure 2a and b, some redundant ZnO nanoparticles could also be found on the surfaces of ZnO

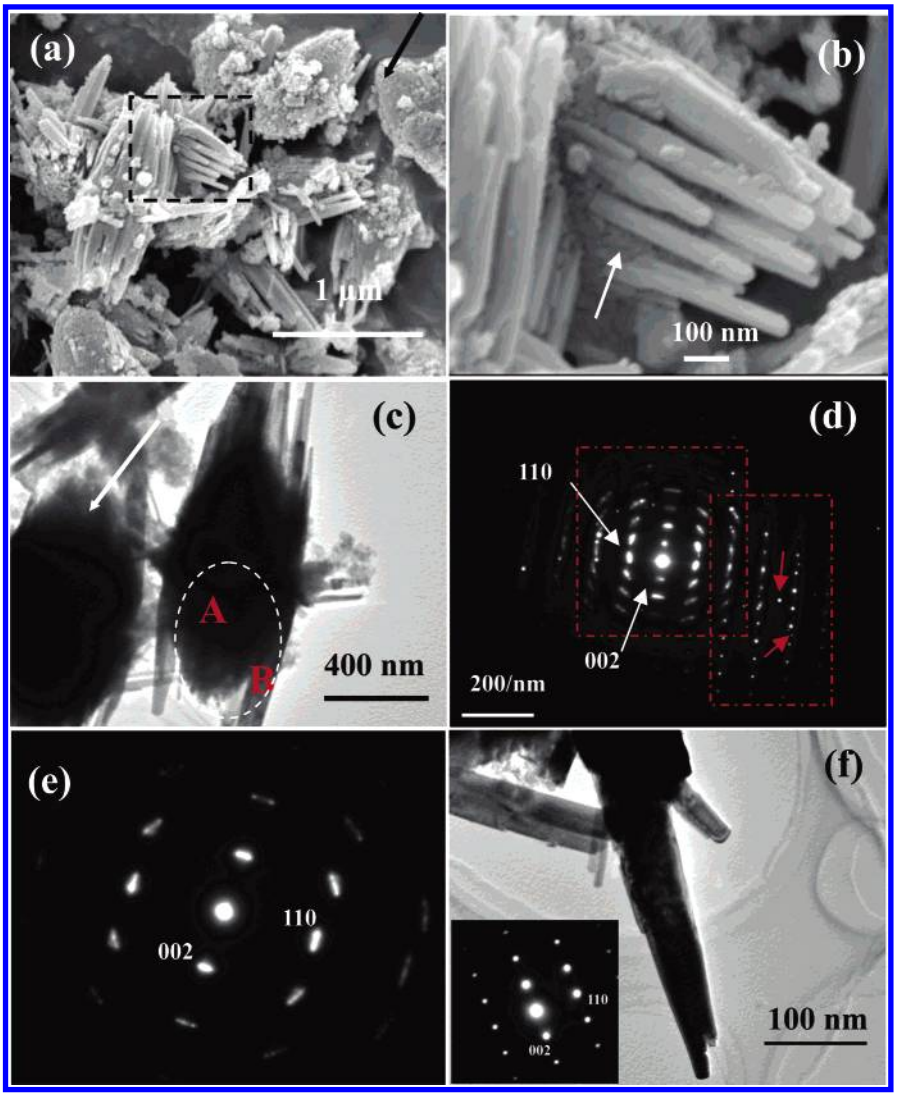

Figure 4. (a) SEM image of underdeveloped ZnO ellipsoids including a few fully developed ones. (b) Enlarged SEM image showing that the ZnO nanoparticles fill in the interspaces of nanorods. (c) TEM image of two underdeveloped ZnO ellipsoids. (d) The SAED pattern taken from one part (marked with a white circle) of the right ellipsoid in Figure 4c. (e) SAED pattern of the left ellipsoid (indicated by a white arrow) in Figure 4c. (f) TEM image and the corresponding SAED pattern of one part of an individual ZnO nanorod.

ellipsoids. However, these redundant particles can be separated easily under strong ultrasonication, indicating that they are not densely packed on the ellipsoidal surfaces. The X-ray energy dispersive spectroscopy (EDS) result shown in Figure 2d demonstrates that the as-prepared sample contains only Zn and O, and the atomic ratio of Zn and O is ~50.55:49.45.

The structure of the ellipsoids was further investigated by TEM. As shown in Figure 3a, a compact standard egg-like morphology and obvious rough surface of the individual ZnO could be observed. The SAED patterns taken from the whole ZnO ellipsoid and one-half of the ellipsoid are shown in Figure 3b and c, respectively. Both parts of the Figure show identical diffraction patterns along the [−1100] direction of ZnO and can also be indexed to the wurtzite structure with phase purity. The growth direction along the long axis of ZnO ellipsoid is [001] (*c* axis). It is interesting and surprising that the assembled structure with micrometer-scale size exhibits an almost single-crystalline diffraction pattern. Further careful examination of Figure 3b and c reveals that some of the diffraction spots (indicated by arrowheads) are arc-like. The slightly broadened and streaked spots demonstrate the presence of few structural defects in the crystal. However, the generation of small misorientation derivating from perfect alignment between nanocrystallines should be reasonable in order to form ellipsoidal microstructure.

The more exciting phenomenon is shown successfully by the characterizations of the early stage of ZnO growth (after 12 h). In the early stage of the growth of ZnO ellipsoids, a large amount of ZnO bundles composed of nanorods and nanoparticles are interestingly observed. Figure 4a reveals the SEM image of underdeveloped ZnO ellipsoids. The result tells us that every individual underdeveloped ZnO consists of ZnO nanoparticles and parallel-arranged ZnO nanorods. The laterally fused rods have diameters in the range of 30−100 nm and lengths of 1−1.5 μm. Furthermore, both ends of the nanorods have relatively smaller diameters compared with the central parts, showing an obvious trend of attaching to each other to form the ellipsoid-like shape. Although most of the products are underdeveloped ZnO ellipsoids, fully developed ZnO ellipsoids similar to that shown in Figure 2 and aggregate particles are observed occasionally (see the arrow-marked spots in Figure 4a). The enlarged image of the area marked with a black rectangle is shown in Figure 4b. It could be observed that ZnO nanoparticles fill in the voids among the nanorods densely. In addition, the average size of these nanoparticles is consistent with the surface-particle size in the final ZnO ellipsoidal architectures. Figure

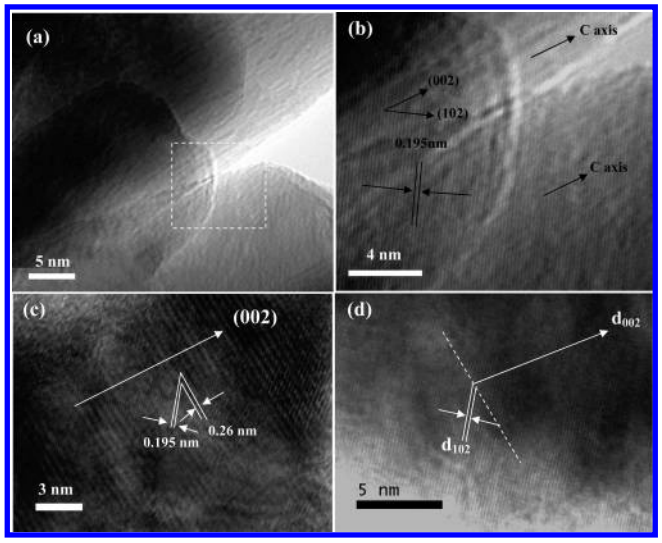

Figure 5. (a) Enlarged TEM image of three adjacent ZnO nanorods from one underdeveloped ellipsoid. (b) The HRTEM image of the connecting area labeled by a rectangle in Figure 5a, indicating that these rods share the same 3D orientation. (c) HRTEM image of some nanoparticles in the underdeveloped ZnO ellipsoid. (d) HRTEM image taken from the edge area of one fully developed ellipsoid.

4c shows the TEM image of two underdeveloped ZnO ellipsoids. Figure 4d is the corresponding SAED pattern taken from the area marked with a white circle in Figure 4c. The diffraction pattern, containing more elongated spots, could also be approximately indexed to a single-crystal structure with *c* axis orientation. From careful examination, one can find that the mentioned SAED pattern is in fact the superposition of two similar individual ones, as illustrated by red rectangles in Figure 4d. The misorientation between the two series of SAED patterns is estimated to be ~3°. The diffraction pattern on the right-hand side can be assigned to the nanorods in the B area in Figure 4c, while the pattern on the left-hand side is recorded from the A area. It is worth mentioning that some additional diffraction spots indicated by red arrows in Figure 4d should be attributed to the dispersed or aggregate nanoparticles that are adsorbed on the surface of ZnO ellipsoid and not arraying along the [001] crystallographic direction. The SAED pattern of the left-hand underdeveloped ZnO ellipsoid in Figure 4c is shown in Figure 4e. It can also be assigned to quasi-single-crystal structure with the long axis along the [001] direction. Figure 4f is a TEM image of one part of a ZnO nanorod from an underdeveloped ellipsoid. The corresponding bright SAED pattern indicates that the ZnO nanorods are single crystals and grow along the [001] orientation, which is in agreement with the one-dimensional anisotropic growth habit of ZnO crystals.[4,5,13]

All of the above results give evidence that the final anisotropic ellipsoidal architecture is formed from the oriented attachment of nanoparticles and nanorods. The HRTEM examinations displayed below further support this conclusion. Figure 5a shows the enlarged TEM image of three ZnO nanorods from one underdeveloped ellipsoid. The HRTEM image of the area marked by a rectangle is demonstrated in Figure 5b. The three nanorods contact very closely and form a structurally uniform single crystal. The parallelism and overlap of the lattice fringes demonstrate that the crystallographic axes of all the rods are parallel, providing direct evidence for the oriented-attachment growth mechanism.[9,15] The lattice interplanar spacing is determined to be 0.195 nm, corresponding to the (102) plane of hexagonal ZnO. This suggests that the growth direction of ZnO nanorods is the *c* axis ([001]), as shown in Figure 5b. Figure 5c shows the HRTEM image of some ZnO nanoparticles in the

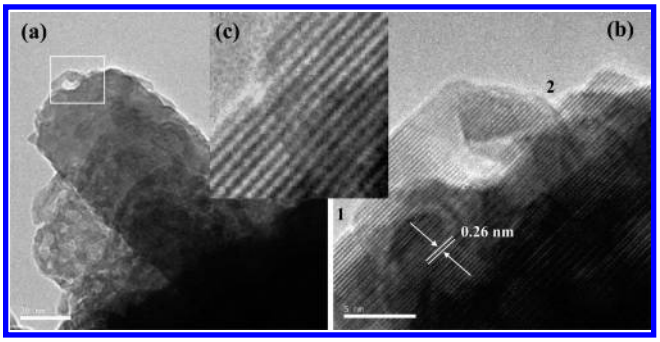

Figure 6. (a) TEM image of one nanorod covered with some nanoparticles in the underdeveloped ellipsoid; (b) HRTEM image of the head part of ZnO nanorod (indicated by a rectangle in a), showing the grain boundaries between the particle and the growing rod. 1 and 2 indicate two obvious boundaries; the scale bars in a and b are 20 and 5 nm, respectively. (c) Enlarged picture of boundary 1, indicating a dislocation (slight waved lattice) induced by imperfectly oriented attachment.

underdeveloped ZnO ellipsoid. The result shows that the crystal growth of these particles occurs along the [001] direction. The lattice spaces can be determined to be 0.195 and 0.26 nm, corresponding to the (102) and (002) planes, respectively. Although the obvious interfaces between nanoparticles could not be seen clearly in this picture, structural defects such as dislocations can be observed in some regions, characteristic of coarsening growth due to imperfectly oriented attachment.[15,16,25] Other HRTEM examinations taken from a relatively large area of nanoparticles in other underdeveloped ellipsoids also demonstrate similar results (see the Supporting Information). However, HRTEM images of orientedly attached ZnO nanoparticles containing obvious interfaces are further provided in the Supporting Information. Figure 5d is a HRTEM image taken from the edge area of one fully developed ZnO ellipsoid. A rough surface can be observed, and the *c* axes of these nanoparticles are also along the growth direction of ZnO ellipsoids. Rougher and obvious particle-assembled surfaces can also be found by HRTEM (see the Supporting Information), which coincides with the SEM results. However, in the inner surface space, there is still no obvious interface between two subunit particles. We therefore propose that the formation process of ZnO ellipsoids includes first oriented attachment and then coarsening.

In the underdeveloped ellipsoids, particle-covered nanorods can also be observed by TEM examination (different from that shown in Figure 5a). Figure 6a shows the TEM image of one ZnO rod covered with some particles. The HRTEM image of the head part (indicated by a rectangle) of this ZnO nanorod is shown in Figure 6b. The single-crystal structure and interplanar spacing of 0.26 nm corresponding to the (002) plane can be seen clearly. In addition, the grain boundaries between the ZnO particle and the growing nanorod is observed and, for example, indicated by 1 and 2. The microscopic grain boundaries and the dislocation shown in Figure 6c (waved lattice, enlarged image of boundary 1) are indicative of crystal formation via association/attachment of nanoparticles and growing ellipsoid rather than via crystal growth.[15,19b]

Growth Process and Mechanism. The overall reaction can be described as follows:[13]

$$Zn(OH)_4^{2-} \xrightarrow{\text{PEG+heating}} ZnO$$

ZnO is a polar crystal; it can be described as a number of tetrahedrally coordinated O^{2-} and Zn^{2+} ions stacking alterna-

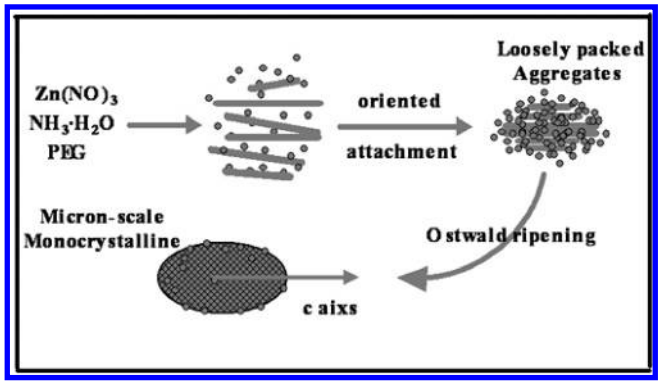

Figure 7. Schematic illustration of the formation and shape evolution of ZnO ellipsoid in the whole synthetic process.

tively along the *c* axis, exhibiting a positive polar plane that is rich in Zn and a negative polar plane that is rich in O. Its growth habit under solution condition has been widely investigated.[5,9−15,24,26] It is accepted that the final morphology of ZnO crystals is related to both their intrinsic crystal structure and external factors, such as surfactants and solvents.[5,8c] The [0001] direction is generally reported to have the highest growth rate; thus, ZnO prefers to grow or assemble into an elongated shape along the *c* axis if there is high monomer concentration in solution.[13d] Although the oriented-attachment mechanism can control the formation of rather complex anisotropic structures,[19] organic molecules such as surfactants also act as surface ligands and have the ability to control the shape and size of the growing nanostructures.[5,11a,13d,13e,13g,15] In addition, with the assistance of surfactants that are adsorbed preferentially in specific planes of inorganic crystals, the oriented-attachment mechanism seems to be a more effective way of producing anisotropic structures.[19a,25] On the basis of the investigations described above, it is possible to interpret the formation process, as shown in Figure 7. First, ZnO nanoparticles and nanorods were formed through conventional nucleation and a subsequent crystal gowth process, relating to both the anisotropic crystal structure of ZnO and the surfactant-involved solution conditions. Then, the nanorods aligned along the *c* axis and the nanoparticles filled the blanks among the rods and covered the surfaces. With further rotation of adjacent nanoparticles and nanorods to share the same 3D crystallographic orientation and subsequent coalescence between these building blocks, loosely aggregated ellipsoidal structures were formed. Finally, the loose aggregates further crystallized and became compact gradually through Ostwald ripening (i.e., coarsening). In a previous report,[19b] SnO_2 nanoparticles and nanobelts were also combined by this oriented-attachment mechanism to reduce the surface and grain boundaries' free energies and generate thermodynamically stable configurations.

As we know, an aggregation process involving the formation of larger crystals by greatly reducing the interfacial energy of small primary nanocrystals is energetically favored. However, the interactions between unprotected building units with nanoscale size are generally not competent to form stable and uniform microstructures,[14,16,25] such as the 3D ellipsoids discussed here. Moreover, the building blocks would always randomly aggregate into disordered crystals rather than single crystals in the absence of sufficiently strong surface-protecting layers.[25] Therefore, in the work reported here, the presence of water-soluble long-chain surfactant PEG, which is adsorbed easily at the surface of metal oxide colloid,[5a] was supposed to be crucial for the formation of this unique self-assembled pattern of ellipsoids. Selective adsorption of PEG molecules on different crystal planes of ZnO nanorods and nanoparticles might take place at first, which could make the primary nanoparticles and nanorods sufficiently stable in the solution, and thus prevent the occurrence of random aggregation. Accordingly, the interaction between surface-adsorbed ligands was believed to be the driving force of self-organization.[14,16,25]As demonstrated by SEM and TEM results, the size scales and particle numbers of the as-synthesized ellipsoids are different in the *c* axis and other crystallographic directions. This typical anisotropic aggregation process should be due to different driving forces in all of the spatial dimensions. Because controlled removal of the appropriate organic ligands at interfaces might provide the capability for subsequent oriented attachment of building blocks to form ordered structures,[16,17,25] proper binding affinity of ligands to metal ions is undoubtedly very important. In the present case, it was believed that PEG were adsorbed relatively more sparsely in the *c* axis direction, which enabled PEG ligands to remove from crystal plane more easily, resulting in preferential assembly growth along this particular orientation. Previously, research results demonstrated that the {100} planes rather than (002) of ZnO could be adsorbed more easily by surfactants such as PEG and PVP.[5a,13g,26] It therefore supports our above conclusion. After the oriented-attachment step, the nanoparticles and nanorods coarsened to some extent through the well-known Ostwald ripening process and the loose "raw" structures were gradually transformed into densely packed ones. Because the coarsening process is generally driven by the system's chemical potential, which decreases with increasing particle size, even though the nanoparticles and nanorods in the inner space of ellipsoids could undergo coarsening due to the equilibrium solute concentration gradients between smaller nonaggregated nanocrystals and larger aggregated ones,[27] this effect might be not obvious when the size of ellipsoidal structure exceeded the critical value. Therefore, some particle-assembled surfaces can still be observed, as shown in Figure 2c. In the work reported here, Ostwald ripening to some extent assisted the process of oriented attachment in yielding finally stable ZnO ellipsoids.

A control experiment has shown that without PEG no ZnO ellipsoids were formed (see the Supporting Information). In addition, if PEG with a lower M_w (PEG-600) was used in our synthetic process, then only irregular flowerlike ZnO structures were obtained. Occasionally, an unformed ZnO ellipsoidal microstructure was observed in the products; the inner parts of that ellipsoid consisted of nanoparticles, while the surface was covered by densely arranged nanorods with very small aspect ratios (see the Supporting Information). It was therefore believed that the chain length of the PEG molecules was also very important to the complex ellipsoidal microstructures. Besides all of the aspects discussed above, the 1D geometrical shape of ZnO nanorods might facilitate the three-dimensionally parallel-alignment along the fixed *c* axis orientation.[12] The stepwise organization and the relatively prolonged time should be beneficial to the compactness of the final structures.

Our finding is very interesting because crystal growth by oriented attachment of two different kinds of building blocks, that is, nanoparticles and nanorods, into 3D micrometer-sacle sized monocrystalline structures could be observed at a low temperature. Further control experiments (such as changing the growth temperature and the amount of ammonia) and their potential implications are under investigation.

Optical Properties Measurement. Several optical studies (Raman, UV−vis absorption, and PL spectra) were carried out to evaluate the crystallization degree and potential optical properties of the as-prepared ZnO ellipsoids. It is well known that hexagonal ZnO has characteristic Raman peaks due to C_{6v}

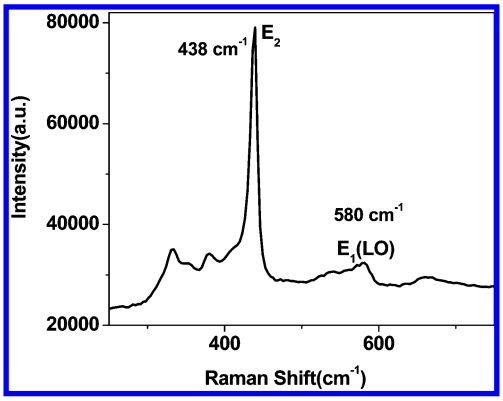

Figure 8. Raman spectrum of the as-prepared ZnO ellipsoids.

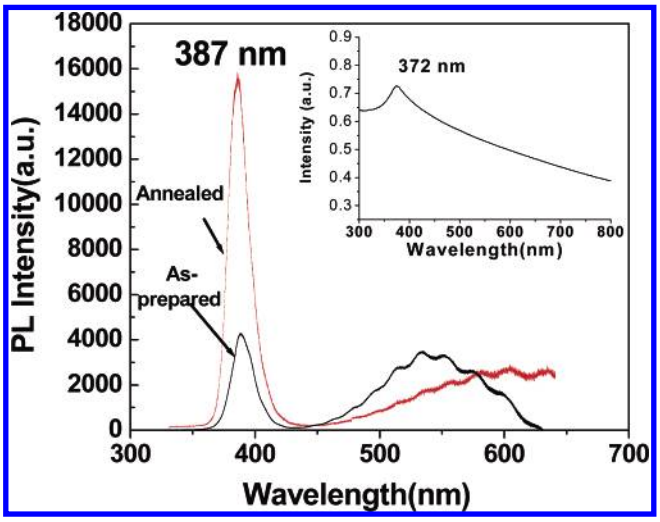

Figure 9. Room-temperature PL spectra recorded from the as-prepared and annealed ZnO ellipsoids. The insert is the UV−vis absorption spectrum of as-prepared ZnO.

symmetry. Single-crystalline wurtzite ZnO has eight sets of optical phonon modes at the Γ point of the Brillouin zone, in which the $A_1 + E_1 + 2E_2$ modes show Raman activity. In addition, the A_1 and E_1 modes split into longitudinal (LO) and transverse (TO) optical components.[5a,6] The Raman spectrum of the ZnO ellipsoids is shown in Figure 8. Among the eight detected peaks, the remarkable peak at 438 cm^{-1} is the nonpolar optical phonon E_2 mode, corresponding to band characteristic of wurtzite phase. The appearance of the longitudinal optical (E_1 LO, 580 cm^{-1}) mode is attributed to the formation of oxygen vacancy, or other defect states. Other relatively high peaks at 332, 380, and 664 cm^{-1} can be assigned to $3E_{2H}-E_{2L}$, A_{1T}, and $2(3E_{2H}-E_{2L})$ modes, respectively.[6a] All of the observed spectroscopic peaks agree well with the literature values[3d,5a,6,11c] and indicate that the obtained monocrystalline ellipsoid has a wurtzite ZnO structure.

For the UV−vis absorption measurement, the as-grown ZnO powders were ultrasonically dispersed in distilled water before examination. The obtained spectrum is inserted in Figure 9. The excitonic absorption peak is centered at ∼372 nm with the calculated band gap of 3.35 eV, which is almost in accordance with the value of bulk ZnO.[5a,11c]

The room-temperature PL spectrum recorded from the dried powder (Figure 9) shows that the ellipsoidal ZnO crystals display an intensive ultraviolet emission peak at ∼387 nm and a relatively weak and broad green light emission peak at ∼530 nm. It is well known that the UV emission peak usually originates from a near-band-edge (NBE) transition of the wide band gap.[6a,13a] The impurities and structural defects, such as oxygen vacancies and so forth, are responsible for the deep level or trap-state emission in the visible range.[6] It is therefore generally accepted that the green emission originates from the radiative recombination of a photogenerated hole with an electron occupying the oxygen vacancy.[3−6,11c,24] In the present case, the 530 nm emission is not negligible. This indicates that there are oxygen vacancies or structural defects in the ZnO self-assembled ellipsoids, which is in good agreement with the HRTEM and Raman results. Similarly, Gui et al.[24] have reported that in the oriented-attachment process of ZnO nanoparticles into nanoribbons the oriented textured particles also induced oxygen vacancies and defects in the final products. For comparison, we further recorded the PL spectrum of ZnO ellipsoids that had been annealed in air at 300 °C for 2 h (red curve in Figure 9). It is worth mentioning that the morphology of ZnO crystals after annealing is unchanged. After the treatment, while the intensity of the UV emission increases dramatically without changing its position, the intensity of the deep-level emission band decreases, indicating an improved crystal quality on annealing. However, the green emission is red-shifted to ∼640 nm. This yellow emission has been related to the interstitial O_i^- in ZnO according to previous work.[28] Why does the heat treatment introduce a new defect (interstitial O_i^-) into the crystals, although the concentration of that defect is very low? Because the evolution of green and yellow bands in ZnO is competitive with each other,[28b] the anneal conditions should be responsible for the weak yellow emission. We consider that there should be an optimal anneal time or temperature, and in that case, the UV emission could be more enhanced while the deep-level emission might be suppressed completely. Further work is now under study.

Conclusions

In summary, monocrystalline ZnO ellipsoidal structures were synthesized successfully by the solution phase method at a really low temperature. The experimental results demonstrated that these self-assembled microstructures composed of nanoparticles and orientationally aligned nanorods were formed by the oriented-attachment mechanism. PEG was of great importance in the formation process. The optical properties of the as-prepared products were also discussed. The understanding of this two-building blocks-involved oriented attachment will be helpful in controllably designing new nano/microstructures for various applications.

Acknowledgment. We gratefully acknowledge financial support from the National Natural Science Foundation of China (no. 50202007). We are appreciative of the valuable suggestions from the referee for the revision of this paper.

Supporting Information Available: HRTEM image of a relatively large area of ZnO nanoparticles in an underdeveloped ellipsoid (a); HRTEM images of assembled particles with obvious grain boundaries (b and c); HRTEM images of the edge area of obvious particle-assembled surface in a fully developed ellipsoid (d and e); FESEM images of ZnO crystals obtained without PEG (f) and using PEG-600 (g and h). This material is available free of charge via the Internet at http://pubs.acs.org.

References and Notes

(1) Choi, K.-S.; Lichtenegger, H. C.; Stucky, G. D.; McFariand, E. W. *J. Am. Chem. Soc.* **2002**, *124*, 12402.
(2) Gao, P. X.; Wang, Z. L. *J. Am. Chem. Soc.* **2003**, *125*, 11299.
(3) (a) Wang, X. D.; Summers, C. J.; Wang, Z. L. *Nano Lett.* **2004**, *4*, 423. (b) Shen, G. Z.; Bando, Y.; Lee, C. J. *J. Phys. Chem. B* **2005**, *109*,

10578. (c) Shen, G. Z.; Bando, Y.; Lee, C. J. *J. Phys. Chem. B* **2005**, *109*, 10779. (d) Han, X. H.; Wang, G. Z.; Jie, J. S., Choy, W. C. H.; Luo, Y.; Yuk, T. I.; Hou, J. G. *J. Phys. Chem. B* **2005**, *109*, 2733.

(4) Huang, M.; Mao, S.; Feick, H.; Yan, H.; Wu, Y.; Kind, H.; Weber, E.; Russo, R.; Yang, P. *Science* **2001**, *292*, 1897.

(5) (a) Li, Z.; Xiong, Y.; Xie, Y. *Inorg. Chem.*, **2003**, *42*, 8105. (b) Zhang, H.; Yang, D. R.; Ma, X. Y.; Que, D. L. *J. Phys. Chem. B* **2005**, *109*, 17055.

(6) (a) Chen, S. J.; Liu, Y. C.; Shao, C. L.; Mu, R.; Lu, Y. M.; Zhang, J. Y.; Shen, D. Z.; Fan, X. W. *Adv. Mater.* **2005**, *17*, 586. (b) Shen, G. Z.; Bando, Y.; Liu, B. D.; Golberg, D.; Lee, C. J. *Adv. Fuct. Mater.* **2006**, *16*, 410.

(7) Pan, Z. W.; Dai, Z. R.; Wang, Z. L. *Science* **2001**, *291*, 1947.

(8) (a) Li, Q. C.; Kumar, V.; Li, Y.; Zhang, H. T.; Marks, T. J.; Chang, R. P. H. *Chem. Mater.* **2005**, *17*, 1001. (b) Li, P.; Wei, Y.; Liu, H.; Wang, X. *Chem. Commun.* **2004**, *10*, 2856. (c) Liu, J. P.; Huang, X. T. *J. Solid State Chem.* **2006**, *179*, 843.

(9) Pacholski, C.; Kornowski, A.; Weller, H. *Angew. Chem., Int. Ed.* **2002**, *41*, 1188.

(10) Tian, Z. R.; Voigt, J. A.; Liu, J.; Mckenzie, B.; Mcdermott, M. J. *J. Am. Chem. Soc.* **2002**, *124*, 12954.

(11) (a) Li, F.; Ding, Y.; Gao, P.; Xin, X.; Wang, Z. L. *Angew. Chem.* **2004**, *116*, 5350. (b) Xu, L. F.; Guo, Y.; Liao, Q.; Zhang, J. P.; Xu, D. S. *J. Phys. Chem. B* **2005**, *109*, 13519. (c) Liang, J. B.; Liu, J. W.; Xie, Q.; Bai, S.; Yu, W. C.; Qian, Y. T. *J. Phys. Chem. B* **2005**, *109*, 9463. (d) Cao, B. Q.; Cai, W. P.; Li, Y.; Sun, F. Q.; Zhang, L. D. *Nanotechnology* **2005**, *16*, 1734.

(12) (a) Liu, B.; Zeng, H. C. *J. Am. Chem. Soc.* **2004**, *126*, 16744. (b) Liu, B.; Zeng, H. C. *J. Am. Chem. Soc.* **2003**, *125*, 4430.

(13) (a) Cao, J. M.; Wang, J.; Wang, B. Q.; Chang, X.; Zheng, M. B.; Wang, H. Y. *Chem. Lett.* **2004**, *33*, 1332. (b) Wang, W. W.; Zhu, Y. J. *Chem. Lett.* **2004**, *33*, 988. (c) Sun, X. H.; Lam, S.; Sham, T. K.; Heigl, F.; Jurgensen, A.; Wong, N. B. *J. Phys. Chem. B* **2005**, *109*, 3120. (d) Zhang, H.; Yang, D. R.; Ma, X. Y.; Ji, Y. J.; Xu, J.; Que, D. L. *Nanotechnology* **2004,** *15*, 622. (e) Gao, X. D.; Li, X. M.; Yu, W. D. *J. Phys. Chem. B* **2005**, *109*, 1155. (f) Qian, H. S.; Yu, S. H.; Gong, J. Y.; Luo, L. B.; Wen, L. L. *Cryst. Growth Des.* **2005**, *5*, 935. (g) Liu, J. P.; Huang, X. T.; Duan, J. X.; Ai, H. H.; Tu, P. H. *Mater. Lett.* **2005**, *59*, 3710.

(14) Gao, X. P.; Zheng, Z. F.; Zhu, H. Y.; Pan, G. L.; Bao, J. L.; Wu, F.; Song, D. Y. *Chem. Commun.* **2004**, *12*, 1428.

(15) Mo, M. S.; Yu, J. C.; Zhang, L. Z.; Li, S. A. *Adv. Mater.* **2005**, *17*, 756.

(16) Penn, R. L.; Banfield, J. F. *Science* **1998**, *281*, 969.

(17) Tang, Z.; Kotov, N. A.; Giersig, M. *Science* **2002**, *297*, 237.

(18) Liu, B.; Zeng, H. C. *J. Am. Chem. Soc.* **2004**, *126*, 8124.

(19) (a) Lee, E. J. H.; Ribeiro, C.; Longo, E.; Leite, E. R. *J. Phys. Chem. B* **2005**, *109*, 20842. (b) Ribeiro, C.; Lee, E. J. H.; Giraldi, T. R.; Aguiar, R.; Longo, E.; Leite, E. R. *J. Appl. Phys.* **2005**, *97*, 024313. (c) Ribeiro, C.; Lee, E. J. H.; Longo, E.; Leite, E. R. *ChemPhysChem* **2005**, *6*, 690.

(20) Adachi, M.; Murata, Y.; Takao, J.; Jiu, J. T.; Sakamoto, M.; Wang F. M. *J. Am. Chem. Soc.* **2004**, *126*, 14943.

(21) Vayssieres, L.; Graetzel, M. *Angew. Chem., Int. Ed.* **2004**, *43*, 3666.

(22) (a)Yu, J. H.; Joo, J.; Park, H. M.; Baik, S. I.; Kim, Y. W.; Kim, S. C.; Hyeon, T. *J. Am. Chem. Soc.* **2005**, *127*, 5662. (b) Cho. K. S.; Talapin, D. V.; Gaschler, W.; Murray, C. B. *J. Am. Chem. Soc.* **2005**, *127*, 7140.

(23) Niederberger, M.; Krumeich, F.; Hegetschweiler, K.; Nesper, R. *Chem. Mater.* **2002**, *14*, 78.

(24) Gui, Z.; Liu, J.; Wang, Z. Z.; Song, L.; Hu, Y.; Fan, W. C.; Chen, D. Y. *J. Phys. Chem. B* **2005**, *109*, 1113.

(25) Zhang, Z.; Sun, H.; Shao, X.; Li, D.; Yu, H.; Han, M. *Adv. Mater.* **2005**, *17*, 42.

(26) (a) Tao, D. L.; Qian, W. Z.; Huang, Y.; Wei, F. *J. Cryst. Growth* **2004**, *271*, 353. (b) Liu, X. M.; Zhou, Y. C. *J. Cryst. Growth* **2004**, *270*, 527. (c) Liu, J. P.; Huang, X. T.; Li, Y. Y.; Duan, J. X.; Ai, H. H.; Ren, L. *Mater. Sci. Eng., B* **2006**, *127*, 85.

(27) Sugimoto, T. *Adv. Colloid Interface Sci.* **1987**, *28*, 65.

(28) (a) Wu, X. L.; Siu, G. G.; Fu, C. L.; Ong, H. C. *Appl. Phys. Lett.* **2001**, *78*, 2285. (b) Pal, U.; Santiago, P. *J. Phys. Chem. B* **2005**, *109*, 15317.